Impact of detubulation on force and kinetics of cardiac muscle contraction

Cecilia Ferrantini,[1,2] Raffaele Coppini,[1,2,3] Leonardo Sacconi,[4,6] Benedetta Tosi,[1,2] Mei Luo Zhang,[7] Guo Liang Wang,[7] Ewout de Vries,[7] Ernst Hoppenbrouwers,[7] Francesco Pavone,[4,5,6] Elisabetta Cerbai,[1,2,3] Chiara Tesi,[1,2] Corrado Poggesi,[1,2] and Henk E.D.J. ter Keurs[7]

[1]Center of Molecular Medicine, [2]Department of Experimental and Clinical Medicine, Division of Physiology, [3]Department of NeuroFarBa, Division of Pharmacology, [4]LENS, European Laboratory for Non-Linear Spectroscopy, and [5]Department of Physics, University of Florence, 50121 Florence, Italy
[6]National Institute of Optics, National Research Council, 50019 Sesto Fiorentino, Italy
[7]Department of Cardiac Sciences of the Libin Institute at the Faculty of Medicine, University of Calgary, Calgary, Alberta T2N 1N4, Canada

Action potential–driven Ca^{2+} currents from the transverse tubules (t-tubules) trigger synchronous Ca^{2+} release from the sarcoplasmic reticulum of cardiomyocytes. Loss of t-tubules has been reported in cardiac diseases, including heart failure, but the effect of uncoupling t-tubules from the sarcolemma on cardiac muscle mechanics remains largely unknown. We dissected intact rat right ventricular trabeculae and compared force, sarcomere length, and intracellular Ca^{2+} in control trabeculae with trabeculae in which the t-tubules were uncoupled from the plasma membrane by formamide-induced osmotic shock (detubulation). We verified disconnection of a consistent fraction of t-tubules from the sarcolemma by two-photon fluorescence imaging of FM4-64–labeled membranes and by the absence of tubular action potential, which was recorded by random access multiphoton microscopy in combination with a voltage-sensitive dye (Di-4-AN(F)EPPTEA). Detubulation reduced the amplitude and prolonged the duration of Ca^{2+} transients, leading to slower kinetics of force generation and relaxation and reduced twitch tension (1 Hz, 30°C, 1.5 mM $[Ca^{2+}]_o$). No mechanical changes were observed in rat left atrial trabeculae after formamide shock, consistent with the lack of t-tubules in rodent atrial myocytes. Detubulation diminished the rate-dependent increase of Ca^{2+}-transient amplitude and twitch force. However, maximal twitch tension at high $[Ca^{2+}]_o$ or in post-rest potentiated beats was unaffected, although contraction kinetics were slower. The ryanodine receptor (RyR)2 Ca-sensitizing agent caffeine (200 µM), which increases the velocity of transverse Ca^{2+} release propagation in detubulated cardiomyocytes, rescued the depressed contractile force and the slower twitch kinetics of detubulated trabeculae, with negligible effects in controls. We conclude that partial loss of t-tubules leads to myocardial contractile abnormalities that can be rescued by enhancing and accelerating the propagation of Ca^{2+}-induced Ca^{2+} release to orphan RyR2 clusters.

The Journal of General Physiology

INTRODUCTION

Transverse tubules (t-tubules) are invaginations of the surface membrane that occur at each Z-line and carry electrical excitation to the core of cardiac myocytes. The transverse tubular (TT) system is also called "transverse-axial tubular system" (TATS) for the presence of axial tubules connecting transversal ones (Ferrantini et al., 2013). The key proteins involved in excitation–contraction coupling, such as dihydropyridine receptors and sodium–calcium exchangers (NCXs), are located predominantly on the TATS membranes (Yang et al., 2002; Pásek et al., 2008; Orchard et al., 2009), adjacent to Ca^{2+} release units in the SR. This ensures that Ca^{2+} release occurs synchronously throughout the cell and that Ca^{2+} is extruded rapidly from the myocyte, as no part of the cytoplasm is more than one micrometer apart from the nearest t-tubule and its Ca^{2+} inflow and outflow pathways. Renewed interest in TATS function stems from the fact that loss/disorganization of t-tubules, accompanied by orphaned RyRs (Song et al., 2006), have been found in several pathological conditions, including human congestive heart failure (CHF) (Louch et al., 2004; Lyon et al., 2009) and dilated and hypertrophic cardiomyopathies (Lyon et al., 2009), as well as in animal

C. Ferrantini and R. Coppini contributed equally to this paper.
Correspondence to Cecilia Ferrantini: cecilia.ferrantini@unifi.it

Abbreviations used in this paper: CHF, congestive heart failure; FFT, fast Fourier transform; NCX, sodium–calcium exchanger; RAMP, random access multiphoton; SL, sarcomere length; TATS, transverse-axial tubular system; TPF, two-photon fluorescence; TT, transverse tubular; t-tubule, transverse tubule.

The Rockefeller University Press $30.00
J. Gen. Physiol. Vol. 143 No. 6 783–797
www.jgp.org/cgi/doi/10.1085/jgp.201311125

models of CHF (He et al., 2001; Lyon et al., 2009), chronic ischemia (Heinzel et al., 2008), and atrial fibrillation (Dibb et al., 2009; Lenaerts et al., 2009). All the above conditions are characterized by altered twitch force and kinetics caused by complex remodelling of membrane currents and by SR and myofilament function (Yano et al., 2005). The reduction of TATS density, usually paralleled by increased cell dimensions, can be an additional pathogenic element contributing to mechanical impairment in cardiac diseases. However, reduction of TATS density occurs in all cardiac disease models along with other cellular and extracellular alterations, thus the effect of detubulation by itself on myocardial contractile function cannot be easily assessed. For instance, peak stress was reduced and contractions were slower in failing hypertensive (Ward et al., 2011) and ischemic (Lyon et al., 2009) rat hearts, which clearly exhibited a lower fraction of t-tubules per unit of cell volume. However, in these models, the presence of a shift in myosin iso-enzyme composition (i.e., from α to β myosin heavy chain isoform) may mask much of the mechanical effects of TT loss.

A model of "acute" TT disruption could help to establish a causative effect between loss of TATS and mechanical abnormalities. A technique to physically uncouple the t-tubules from the surface membrane (detubulation) by osmotic shock has been described and validated in isolated ventricular myocytes (Kawai et al., 1999; Brette et al., 2002). However, detailed mechanical measurements have not been performed in detubulated cells, as it is generally difficult to control the loading conditions of isolated myocytes. Previous efforts to detubulate intact cardiac muscles have been unsuccessful (Chapman, 1980; Kawai et al., 1999).

In this work, we used formamide-induced osmotic shock to induce acute detubulation of thin intact cardiac muscle preparations in which mechanical measurements can be performed in highly controlled conditions. We determined how TT loss affects contraction kinetics and force developed by the cardiac muscle at different inotropic levels, and how detubulation alters the dynamics of intracellular Ca^{2+} cycling under physiological mechanical loading.

MATERIALS AND METHODS

Male LBNF1 and Wistar-Han rats (Harlan Laboratories) weighing 250–300 g were used for the experiments, in accord with local regulations for laboratory animal use. Rats were heparinized (5,000 UI/ml) and anesthetized by inhaled isoflurane. We used multicellular preparations and single cardiomyocytes to record force, sarcomere length (SL), and intracellular calcium as detailed below. A subset of trabeculae was used for imaging studies.

Cardiac multicellular preparations

Left atrial and right ventricular trabeculae were selected because of their similarity with fascicles in the cardiac wall (Hanley et al., 1999; Baudino et al., 2006) and dissected from rats as described previously (de Tombe and ter Keurs, 1990). The heart was rapidly excised and placed in a dissection dish beneath a binocular microscope; the proximal aorta was perfused retrogradely with a modified Krebs–Henseleit (KH) solution. KH solution contained (mM): 120 NaCl, 5 KCl, 2 $MgSO_4$, 1.2 NaH_2PO_4, 20 $NaHCO_3$, 0.50 $CaCl_2$, and 10 glucose, pH 7.4, equilibrated with 95% O_2/5% CO_2. During perfusion and dissection, the potassium concentration in the KH solution was raised to 15 mmol/L to stop spontaneous beating. 20 mmol/L butanedione-monoxime (BDM) was also added to the solution to minimize contractures after cutting damage. Thin (50–200-µm diameter) unbranched uniform trabeculae, running between the free wall of the right ventricle and the atrioventricular ring, were selected and carefully dissected by cutting through the atrioventricular ring on one end and removing a portion of the right ventricular wall on the other end. Free running atrial trabeculae were also dissected from the left atrium. In this case, a block of tissue was left at both ends to facilitate mounting.

Force measurements

Ventricular and atrial trabeculae were mounted between a basket-shaped platinum end of a force transducer (KG7A; Scientific Instruments) or a modified silicon strain gauge (AE-801; SenSonor) and a motor (Aurora Scientific Inc.), with both connected to micromanipulators. Muscles were initially perfused with the KH solution without BDM at room temperature and stimulated at 0.5 Hz. Subsequently, baseline conditions were set (1 Hz, 30°C, 1.8 mmol/L [$CaCl_2$]). Muscles were allowed to stabilize for at least 20–30 min before the experimental protocol was initiated. In a subset of experiments, force measurements were combined either with intracellular calcium or SL recordings, performed as described below.

Intracellular calcium measurements

The muscles were loaded with the cell-permeant acetoxymethyl ester form of the fluorescent intracellular Ca^{2+} indicator fura-2 AM (Molecular Probes) (Lamberts et al., 2007). Dissected trabeculae were incubated for 30 min at 37°C in a modified KH solution (containing 1 mM $CaCl_2$ and 10 mM HEPES, pH 7.35 adjusted with NaOH). This solution was supplemented with 10 µM fura-2 AM, 10 µM (−)-blebbistatin (Sigma-Aldrich), and 10 µl/ml PowerLoad Concentrate (100×; Molecular Probes). After 30 min, loaded trabeculae were washed with the same KH solution, devoid of fura-2 AM and PowerLoad Concentrate. Loaded trabeculae were then left at room temperature for 10–15 min to allow for fura-2 AM de-esterification and were finally mounted on the force-recording apparatus. Before starting the recordings, trabeculae were superfused with normal KH solution to wash out blebbistatin. To record intracellular [Ca^{2+}], we focused on the central portion of the trabecula and collected fluorescence signals at 505–555 nm with a photon multiplier (Photon Technology International) from a region measuring ∼500 × 100 µm, using a 10× objective. Excitation light was delivered by a monochromator (Photon Technology International), with alternating illumination at 340 and 380 nm (500 wavelength shifts per second). Background fluorescence was automatically subtracted from the signals obtained during illumination at the two wavelengths. Real-time ratio signal was calculated using the Felix32 acquisition program (Photon Technology International). The system allowed us to obtain 250 ratios per second.

To rule out saturation of Ca^{2+} signals, in a subset of experiments (four trabeculae from two rats), we superfused trabeculae with a solution containing 8 mM [Ca^{2+}] and 10 mM caffeine and stimulated the muscle at 10 Hz for 30 s. Under these conditions, mean ratio values were 3.75 ± 0.32 F_{340}/F_{380}. Notably, these values were ∼2.5 times higher than the highest signals detected during experiments (∼1.5 F_{340}/F_{380} at >30 s after rest beats), indicating that Ca^{2+} signals in our experiments were not saturated.

SL measurements

SL was measured by laser diffraction, as described in detail elsewhere (de Tombe and ter Keurs, 1990). The original diameter of a 15-mW He-Ne laser beam was reduced to 300 µm by a 25-cm focal-length lens placed in front of the laser. For measurement of the angle between the zero-order band and the first-order diffraction, the left first-order diffraction band was projected onto a scanning 512-element photodiode array (Reticon).

The photodiode array was scanned every 0.5 msec. The median position of the first-order intensity distribution (determined by analogue circuitry after correction for the contribution of the zero-order diffraction band and scatter) was converted into a voltage proportional to SL by means of a nonlinear amplifier. The transfer function of this amplifier was adjusted by placement of standard glass calibration gratings in the same position as the muscle. The spatial resolution of the diffractometer was 3 nm.

SL was measured in a region of the muscle close to the stationary ventricular end, which was mounted in the platinum basket of the force transducer. After mounting, the muscles were stretched to a SL of 2.10–2.20 µm. Passive force development at this SL is negligible. During the equilibration period, SL both at rest and during contraction decreases as a result of relaxation of the damaged ends; thus, the muscle was restretched to 2.10–2.20 during the experiment. SL fluctuations occurring together with microscopically visible contractile waves were observed during formamide exposure (Fig. S1).

Experimental protocols

We compared force, SL, and intracellular Ca^{2+} in control trabeculae and detubulated trabeculae at 30°C and 1.5 mmol/L $[Ca^{2+}]_o$, unless otherwise specified. The protocol to achieve acute detubulation through formamide-induced osmotic shock is described in Results.

Different patterns of stimulation were used. We assessed the effects of increasing stimulation frequencies (0.1–7 Hz) on twitch force at 30°C. At each frequency, force was allowed to reach steady state before data were recorded. Stimulation pauses were inserted after the last contraction of a steady series (at 1 Hz) to evaluate post-rest potentiation. Different intervals were used, up to maximal pause duration of 60 s. To quantify after rest potentiation, we compared the amplitude of the first beat after the pause to that of the last beat of the steady-state series. Pharmacological interventions were applied, including 200 µmol/L caffeine as a RyR2 Ca^{2+}-sensitizing agent.

Two-photon fluorescence (TPF) imaging and analysis of TT density

The basic design of our imaging systems has been described previously (Cicchi et al., 2008; Allegra Mascaro et al., 2010). In brief, a mode-locked Ti/sapphire laser (120-fs–width pulses, 90-MHz repetition rate, 900-nm wavelength; Chameleon; Coherent, Inc.) was coupled into a custom-made scanning system based on a pair of galvanometric mirrors (GSI Group Inc.). The laser was focused onto the specimen by an objective lens (20×, NA 0.95, WD 2 mm; XLUM; Olympus). The same objective lens was used for TPF signal collection and the photomultiplier (Hamamatsu) for signal detection. Trabeculae were stained with membrane-selective fluorescent dye (FM4-64; Molecular Probes) through bulk loading (50 µg/ml) either before or after detubulation and were observed at room temperature under the TPF microscope, with an excitation wavelength of 900 nm. Z-stacks of 2-µm sections were acquired, spanning the whole muscle thickness. TATS morphology was analyzed in terms of TT density using a method based on fast Fourier transform (FFT). We quantified the TT density by measuring the 0.50 ± 0.05–μm^{-1} peak component (related to TT periodicity, 1.8–2.2 µm) of the power spectrum of the image. In detail, the fraction of the ∼0.5-μm^{-1} component (TT%) was obtained by normalizing the area under the peak to the total area subtending the power spectrum curve. An open-source imaging-processing software (1.43u; ImageJ) was used to perform the analysis. Examples of FFT images of trabeculae with variable TT density are shown in Fig. S2. TT% was evaluated in six different areas (60 × 30 µm) of each trabecula, and the average value was assumed as mean TT density of the muscle.

Random access multiphoton (RAMP) microscopy and action potential measurements

Trabeculae were loaded with the voltage-sensitive dye Di-4-AN(F)EPPTEA (provided by P. Yan and L.M. Loew, University of Connecticut Health Center, Farmington, CT; Yan et al., 2012), and membrane potential changes were monitored simultaneously from multiple sites using a custom-made RAMP microscope, as described previously (Sacconi et al., 2012). Trabeculae were loaded in HEPES buffer (HB), which contained (mM): 132 NaCl, 4 KCl, 1.2 $MgCl_2$, 10 HEPES, and 10 glucose, pH 7.35 with NaOH. HB for loading also contained: 1 mM $CaCl_2$, 10 µM blebbistatin, and 20 µg/ml di-4-AN(F)EPPTEA. Muscles were incubated for 30 min at room temperature and then resuspended in HB solution with 1 mM $CaCl_2$, 10 µM blebbistatin, and 10–20 µM cytochalasin D. Loaded preparations were used for experiments within 1 h. The excitation was provided by a high power, passively mode-locked fiber laser operating in the 1,064-nm spectral range (Fianium), which comprised 200-fs-width pulses at an 80-MHz repetition rate. The scanning head was developed by using an acousto-optical deflection (AOD) system composed of two AOD systems crossed at 90° (AA Opto-Electronic). The spatial distortion of the laser pulse in the AOD system is known to affect the radial and axial resolutions of the microscope. To compensate for the larger dispersion caused by two crossed AOD systems, we used an acousto-optic modulator (AOM) placed at 45° with respect to the two axes of the AOD systems. We chose the appropriate propagation direction and frequency of the ultrasonic wave in the AOM, which propagates in the opposite direction with respect to the sum of the two waves in the AOD systems. To compensate for the spatial distortion at the center of the field of view (F0), AOM frequency was fixed at a value given by $F0 \cdot \sqrt{2}$. A water-immersion objective (40×, NA 0.8; Olympus) was used in experiments with trabeculae. The fluorescence signal was collected in the backward direction by the excitation objective and in the forward direction using a condenser lens (NA 1.4; Olympus). The fluorescence signal was detected by two independent GaAsP photomultiplier modules (Hamamatsu). Emission filters of 655 ± 20 nm (Semrock, Inc.) were used. The RAMP microscope was capable of commutating between two positions in the focal plane in ∼4 µs. The opto-electronic components of the setup were computer controlled with custom-made software developed in LabVIEW 7.1 (National Instruments). In a typical measurement, we probed 5–10 different sarcolemmal sites (e.g., surface sarcolemma and the t-system of two to three adjacent cells). The integration time per membrane pass for each scanned site was ∼100 µs. The length of the scanned lines ranged from 2 to 10 µm, following the geometry of the probed sarcolemmal domain. The signal to noise ratio (S/N) for real-time optical action potential detection was ∼10.

Confocal imaging to assess CICR transverse propagation velocity on detubulated cardiomyocytes

Single ventricular cardiomyocytes were isolated from rat hearts by enzymatic dissociation using the Langendorff perfusion method, as described previously (Sacconi et al., 2012). The excised heart was immediately bathed in HB, cannulated through the aorta, and perfused with the HB for 3–4 min at a constant flow of 3 ml/min at 37°C. The perfusate was then switched to the enzyme solution (the same HB supplemented with 0.1 mg/ml Liberase TM Research Grade; Roche). The solution was recirculated for 7–8 min. The ventricles were then excised and shredded into several pieces.

Gentle stirring facilitated dissociation of the tissue. The cell suspension was slowly centrifuged, and the cell pellet (~0.1 ml) was resuspended in HB supplemented with 0.1 mM $CaCl_2$ and 1 mg/ml BSA. Calcium concentration was gradually raised up to 0.6 mM. Isolated cells were stored at room temperature (20°C) in HB containing 600 µM $CaCl_2$ and 10 µM blebbistatin. Myocytes were then incubated in HB for 30 min at room temperature after adding 5 µM Fluoforte (Enzo Life Sciences) and 1% Powerload Concentrate (Molecular Probes). Myocytes were finally washed in HB containing 1 mM $CaCl_2$ and 10 µM blebbistatin. Myocyte suspensions were transferred to a recording chamber with field-stimulation electrodes, mounted on a confocal microscope stage (TCS SP5; Leica). The excitation wavelength was 488 nm. Fluoforte fluorescence was detected at 505–545 nm. CICR propagation velocity was measured as the slope ($\Delta x/\Delta t$) in line scan images, while cells were electrically stimulated at 1 Hz via field electrodes. Lines were 30–60 µm in length (mean of 40.74 ± 0.36 µm) to comprise the entire myocyte transverse diameter. Images were acquired with a resolution of 512 pixels/line for 5–6 s, with a scan rate of 750 Hz.

In a subset of experiments, myocytes were loaded with FM4-64 after formamide-induced osmotic shock, and 3-D stacks (0.1–0.3-µm z-axis step) were acquired (setting a field of view of 150 × 150 µm and a resolution of 1,024 × 1,024 pixels) to confirm the occurrence of TT detachment.

Statistics

Statistical analysis was performed using Origin 9.0 software (OriginLab). Student's *t* test for paired values was used to compare control and detubulated trabeculae and to assess the effects of drugs or interventions. A p-value of <0.05 was considered statistically significant. The number of animals and trabeculae tested for each set of measurements is indicated in the text or in the figure legends.

Online supplemental material

Fig. S1 shows the effects of detubulation on diastolic SL and tension–SL relationships. Fig. S2 contains examples of trabeculae with variable TT density. The online supplemental material is available at http://www.jgp.org/cgi/content/full/jgp.201311125/DC1.

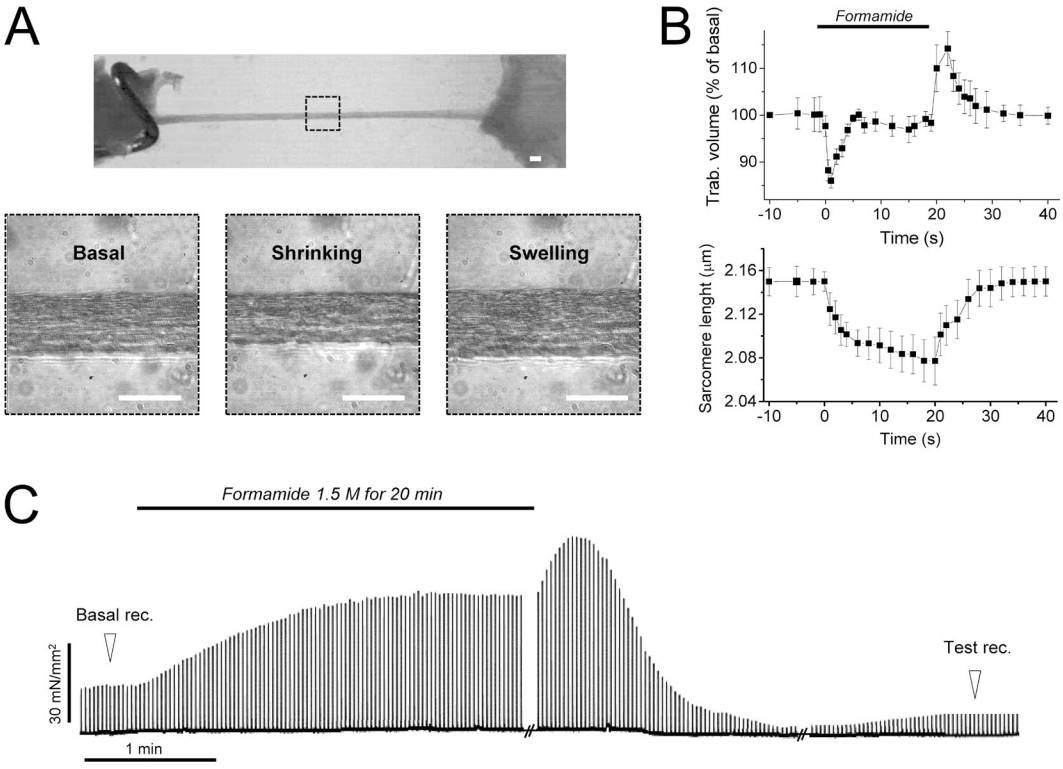

Figure 1. Transient volume, SL, and force changes during formamide-induced osmotic shock. (A) Representative stereomicroscope image of a rat right ventricular trabecula mounted between a force transducer (left, basket) and a motor (right, hook). The highlighted region is displayed below as observed with a 20× microscope objective to show trabecular diameter changes occurring during formamide exposure. Bars, 50 µm. (B; top) Changes in muscle volume versus time during formamide osmotic shock protocol. 1.5 M formamide was applied for 20 min and rapidly removed. Muscle volume is estimated from trabecular width, thickness, and length by assuming the trabeculae to be elliptical cylinders. Values are means ± SE from six trabeculae. (Bottom) SL versus time during formamide shock; means ± SE from seven rat ventricular trabeculae. (C) Representative twitch force changes during the experimental protocol. Twitch active stress increases to a maximum within the first 3 min of formamide exposure (on average by 146 ± 63% in six trabeculae). Twitch force is above the basal level during the entire formamide exposure period and shows a further transient increase during the first 30 s of formamide washout. Subsequently, twitch force decreases to a minimum (47 ± 24% of preexposure level) before attaining a new steady level in 7–8 min. Several mechanisms may contribute to the transient force increase during formamide exposure (e.g., $[Ca^{2+}]_i$ increase and reduced myofilament spacing caused by cell shrinkage, direct effects of formamide on force generation, etc.). However, it appears to be a rather transitory and unspecific event because it occurs both in formamide-treated ventricular and atrial trabeculae (Fig. 5).

RESULTS

Formamide shock in ventricular trabeculae to achieve acute detubulation

Thin rat ventricular trabeculae mounted on the force-recording apparatus and paced at low rates (0.5 Hz, 30°C, 1.5 mmol/L $[Ca^{2+}]_o$) were exposed for 20 min to a hypertonic (1.5 mol/L) formamide-containing buffer, followed by a rapid (<10 s) washout with normal isotonic solution. Muscle volume, SL, and force were monitored during the protocol (Fig. 1).

Muscle volume initially decreased upon exposure to formamide, but this reversed rapidly upon formamide entry into the cells (Fig. 1 A). When formamide-containing solution was rapidly replaced with normal isotonic solution, muscle volume increased (+16.5 ± 3.7%) rapidly (<30 s) and transiently (Fig. 1 B). This rapid volume step is likely to pull and detach t-tubules from the surface membrane. Transient force and SL changes occurred during the osmotic shock procedure (Fig. 1, B and C). Test recordings from each trabecula were performed before and >10 min after formamide exposure (Fig. 1 C).

To test the effectiveness of the detubulation protocol, trabeculae were labeled with the membrane-selective dye FM4-64 and imaged by TPF microscopy (Fig. 2, A–D). Myocytes' dimensions and alignment with the trabecular longitudinal axis were retained after formamide shock, confirming that cellular volume changes are transient. T-tubule density was estimated with an FFT-based method, quantifying the first peak of the spatial frequency components corresponding to TT periodicity (TT component; Fig. S2). Mean TT component was significantly reduced in formamide-treated ventricular trabeculae (0.18 ± 0.06 vs. 0.43 ± 0.04 in untreated trabeculae; $P < 0.01$), indicating the occurrence of TT disconnection from the surface sarcolemma. Atrial trabeculae, known to have a very low density of t-tubules in rodents, were used as negative controls. TPF images of control atrial trabeculae stained with the membrane-selective fluorescent dye FM4-64 showed no t-tubules or a rudimentary TT network (Fig. 2 D), resulting in a mean TT component of 0.03 ± 0.01.

In ventricular trabeculae, the degree of detubulation clearly exhibited a significant intercellular and intracellular variability (Fig. 2, C and E). Such a nonhomogeneous and incomplete TT loss well mimics TT pathological remodeling in heart diseases, where complete TT loss is rarely observed (Lyon et al., 2009). Interestingly, t-tubules do not apparently lose their structural integrity after formamide shock: when the muscles are stained with FM4-64 before formamide exposure, cross-striations are still visible, indicating that t-tubule fragmentation is confined to the subsarcolemmal region while TT structure in the cell core is maintained (Sacconi et al., 2012). This allowed us to test the electrical function of supposedly disconnected t-tubules. Simultaneous optical recordings of surface sarcolemma and t-tubule transmembrane voltage changes (Sacconi et al., 2012) were performed in Di-4-AN(F)EPPTEA–stained trabeculae before and after formamide shock. Of note, the spatial resolution of the system on the z axis (≈1.5 µm) did not allow for detection of the activity of a single t-tubule, but rather, the neighboring TTs located outside the focal plane could contaminate the collected signal. Upon electrical stimulation, t-tubules from formamide-untreated trabeculae always displayed action potentials, with similar

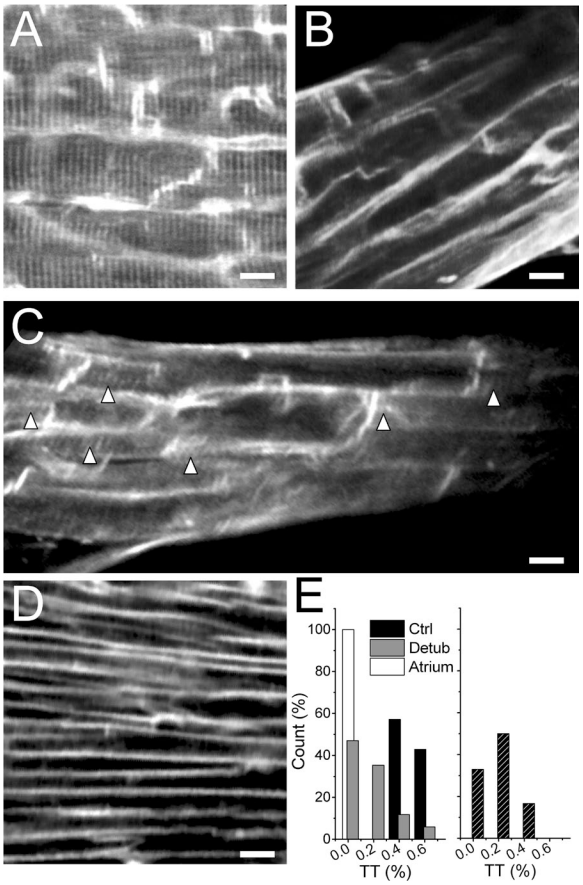

Figure 2. Formamide shock is able to effectively induce acute detubulation of thin rat ventricular trabeculae. (A) TPF image of a control formamide-untreated ventricular trabecula stained with FM4-64, showing a uniform pattern of t-tubules. (B and C) TPF image of ventricular trabeculae stained with FM4-64 after the detubulation protocol. The loss of TT after formamide shock is incomplete: Δ in C indicates residual TT after formamide shock. (D) TPF image of a FM4-64–stained atrial trabecula, in which most of the myocytes show the absence of TT. Bars in A–D, 10 µm. (E; left) Frequency distribution of mean TT component (TT%) obtained by averaging TT% values from six different areas in each trabecula. (Right) Frequency distribution of TT% values in six different areas of a representative detubulated ventricular trabecula. TT% was quantified by FFT analysis of the image. Although the mean TT% is statistically reduced in formamide-treated trabeculae, the effects of formamide shock between different areas can be variable within a single trabecula, ranging from a complete absence of connected T-tubules (TT% of ∼0) to minimal TT disconnection (TT% of >0.4).

shape, amplitude, and timing as those of surface sarcolemma (Fig. 3, A and C). In contrast, t-tubules from detubulated trabeculae displayed a smaller mean voltage variation upon stimulation, in agreement with an overall reduction of the number of functioning TATS elements (Fig. 3, B, D, and E). Additionally, detubulated trabeculae displayed surface sarcolemma action potentials of shorter duration when compared with untreated trabeculae, as expected from a loss of TT L-type Ca^{2+} current ($I_{Ca\text{-}L}$) (Fig. 3 E). This shortening of action potential duration is in agreement with previous observations in detubulated single ventricular cardiomyocytes and indicates that, also in trabeculae, a substantial number of T-tubules are indeed electrically uncoupled from the surface membrane (Sacconi et al., 2012).

Mechanical consequences of acute detubulation: Prolonged contraction kinetics and impaired force–frequency response

Force and Ca^{2+} transient (or SL) were simultaneously measured from isometrically mounted rat ventricular trabeculae stimulated at 1 and 3 Hz before and >10 min after formamide shock. Representative traces are shown in Fig. 4 A. Detubulation reduces steady-state twitch force and slows kinetics of force generation and relaxation. Consistently, Ca^{2+} transient amplitude was reduced, and the kinetics of Ca^{2+} rise and decay were slower (Table 1). Additionally, detubulation hampered the increase of Ca^{2+} transient amplitude and force at a high stimulation rate, whereas the frequency-dependent acceleration of Ca^{2+} and force kinetics was maintained (Fig. 4 B and Table 1). In atrial trabeculae showing a very low TT density in rodents (Fig. 5 A), formamide shock produces similar transient force changes as in the ventricle (Fig. 5 B), but no steady contractile alterations were found compared with baseline (Fig. 5 C and Table 2).

To exclude any nonspecific damage to myofilaments by the osmotic shock, passive and active stress–SL relationships (Hasenfuss et al., 1999) were assessed in rat ventricular trabeculae before and after detubulation. Formamide shock neither affects the passive stress–SL relationship nor the slope of the active stress–SL relationship at a stimulus rate of 1 Hz (Fig. S1). These findings, besides ruling out nonspecific deleterious effects of formamide shock, suggest that t-tubules do not play any major role in the length dependence of cardiac muscle contraction or passive stiffness.

Inotropic interventions in detubulated myocardium: Integrity of maximal force generation capacity and SR content

The following positive inotropic interventions, which were intended to increase SR content, were applied:

(a) Post-rest potentiation. Pauses enhance released Ca^{2+} and developed force by multiple mechanisms, including increased SR Ca^{2+} refilling and enhanced RyR2 channel availability as a result of recovery from inactivation/adaptation during the prolonged diastolic period (Bers et al., 1993; Bassani and Bers, 1994; Maier et al., 2000). Stimulation pauses of variable duration were inserted into a steady-state 1-Hz series (Fig. 6 A). Although the amplitude of Ca^{2+} transients and force twitches at 1 Hz was significantly reduced after detubulation, active

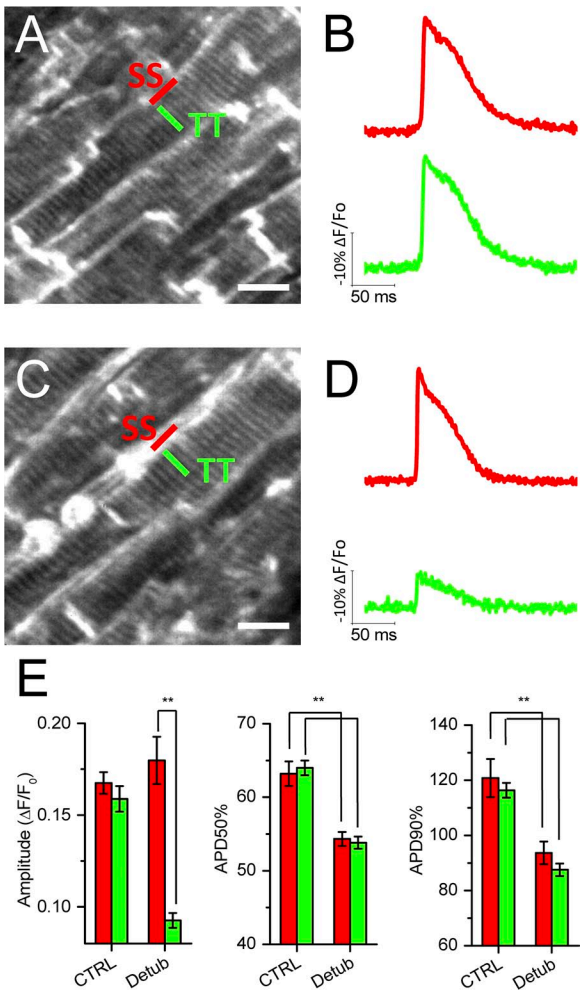

Figure 3. Optical recordings of surface sarcolemma and t-tubule transmembrane voltage confirm TT detachment after formamide shock. (A) TPF image of a Di-4-AN(F)EPPTEA–stained rat ventricular trabecula. Transmembrane voltage at multiple membrane sites was measured with a RAMP microscope. The lines mark the probed sarcolemma regions: surface sarcolemma (SS) is red, and t-tubule (TT) is green. (B) Normalized fluorescence traces from the scanned lines indicated in A. TT and surface sarcolemma action potentials are identical. (C) TPF image of a rat ventricular trabecula after formamide shock: the trabecula was stained before the detubulation procedure. (D) Normalized fluorescence traces from the scanned lines indicated in C: reduced florescence signal is detected in the scanned TATS region, suggesting an electrical uncoupling from surface sarcolemma. (E) Mean ± SE data of fluorescence signal amplitude and action potential duration (in msec) at 50% (APD50%) and 90% (APD90%) of repolarization. Bars, 10 µm. **, $P < 0.01$, paired.

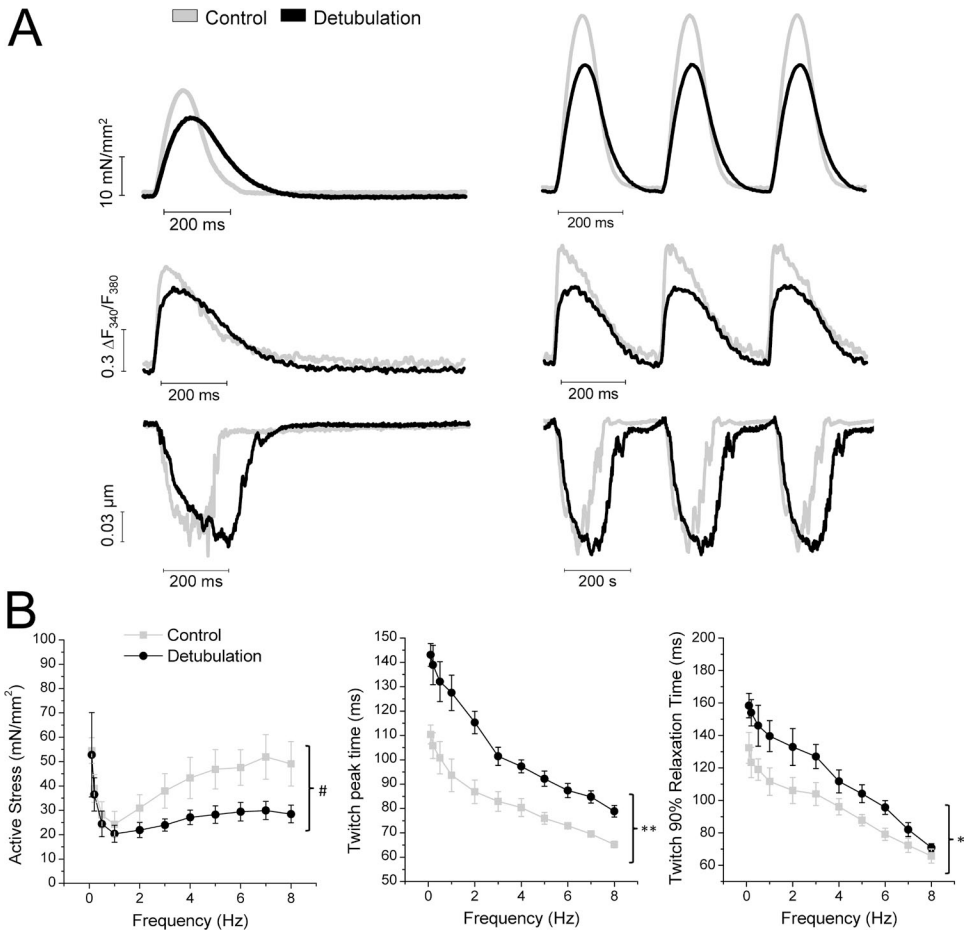

Figure 4. Mechanical consequences of acute detubulation in ventricular trabeculae: prolongation of contraction kinetics and impaired positive force–frequency response. (A) Representative traces of isometric twitch force and corresponding $[Ca^{2+}]_i$ transient at 1- and 3-Hz stimulation frequency before (Control) and after (Detubulation) formamide osmotic shock. $[Ca^{2+}]_i$ was monitored during contraction after loading the trabeculae with fura-2 AM. (B) Steady-state force–frequency relationship and frequency dependency of twitch kinetics in control and detubulated ventricular trabeculae. Data points in the plots represent mean ± SE data of active stress (left), twitch peak time (middle), and 90% relaxation time (right) at frequencies from 0.1 to 8 Hz. Extracellular $[Ca^{2+}]$ was equal to 1.5 mM. n = 8 and 12, number of rats and number of trabeculae, respectively. #, $P < 0.01$, paired t test for frequencies from 1 to 8 Hz; **, $P < 0.01$, paired t test at all frequencies; *, $P < 0.05$, paired t test at all frequencies.

stress developed after a 60-s pause (interval inducing maximum twitch potentiation) was similar before and after formamide shock (Fig. 6 A). Correspondingly, the amplitude of intracellular Ca^{2+} transients of the first beat after a 60-s pause was similar in control and detubulated trabeculae ($\Delta F_{340}/F_{380}$ was 0.91 ± 0.09 vs. 0.84 ± 0.10 in detubulated vs. control, respectively; NS). Nonetheless, the kinetics of post-rest contraction was still slower in detubulated trabeculae (Fig. 6 B), and the underlying post-rest Ca^{2+} transients were still prolonged

TABLE 1

Ventricular trabeculae: Steady-state twitch contractions and $[Ca^{2+}]_i$ transients

Mechanical/calcium parameters	Control	Detubulated	Control	Detubulated
	1 Hz		3 Hz	
Active stress (mN/mm²)	24.3 ± 5.3	20.3 ± 3.5[a]	37.9 ± 7.1	23.9 ± 2.5[b]
Passive stress (mN/mm²)	2.6 ± 0.8	1.3 ± 0.9[b]	3.3 ± 0.9	2.4 ± 1.0[a]
Twitch time to peak (ms)	96 ± 3	131 ± 4[b]	83 ± 3	119 ± 5[b]
Twitch relaxation time 50% (ms)	101 ± 7	119 ± 8[a]	92 ± 5	107 ± 10[a]
Twitch relaxation time 90% (ms)	197 ± 14	227 ± 15[a]	163 ± 8	177 ± 6[b]
Ca^{2+} transients (Δ ratio F_{340}/F_{380})	0.68 ± 0.06	0.55 ± 0.03[a]	0.78 ± 0.06	0.59 ± 0.03[a]
Diastolic $[Ca^{2+}]_i$ (ratio F_{340}/F_{380})	0.59 ± 0.02	0.54 ± 0.03[a]	0.64 ± 0.03	0.57 ± 0.03[a]
$[Ca^{2+}]_i$ time to peak (ms)	36 ± 2	58 ± 3[a]	30 ± 2	52 ± 2[a]
$[Ca^{2+}]_i$ decay time 50% (ms)	144 ± 7	157 ± 7[a]	121 ± 3	127 ± 3[a]
$[Ca^{2+}]_i$ decay time 90% (ms)	247 ± 9	273 ± 10[a]	205 ± 4	226 ± 4[a]

Twitch force and Ca^{2+} transient amplitude and kinetics before and after formamide shock. The time to 50 and 90% relaxation/decay is measured from the peak of the twitch. Temperature was 30°C. Extracellular calcium ($[Ca^{2+}]_e$) was 1.5 mM for force measurements (n = 15 and n = 20) and 1 mM for Ca^{2+} transient measurements (n = 7 and 13, number of rats and number of trabeculae, respectively). At 1 mM $[Ca^{2+}]_e$ (1 Hz), tension was 17.4 ± 2.9 before and 12.2 ± 2.9 after detubulation. $P < 0.05$; contraction kinetics were similar to those at 1.5 mM $[Ca^{2+}]_e$.

[a]$P < 0.05$ in paired Student t test.

[b]$P < 0.01$ in paired Student t test.

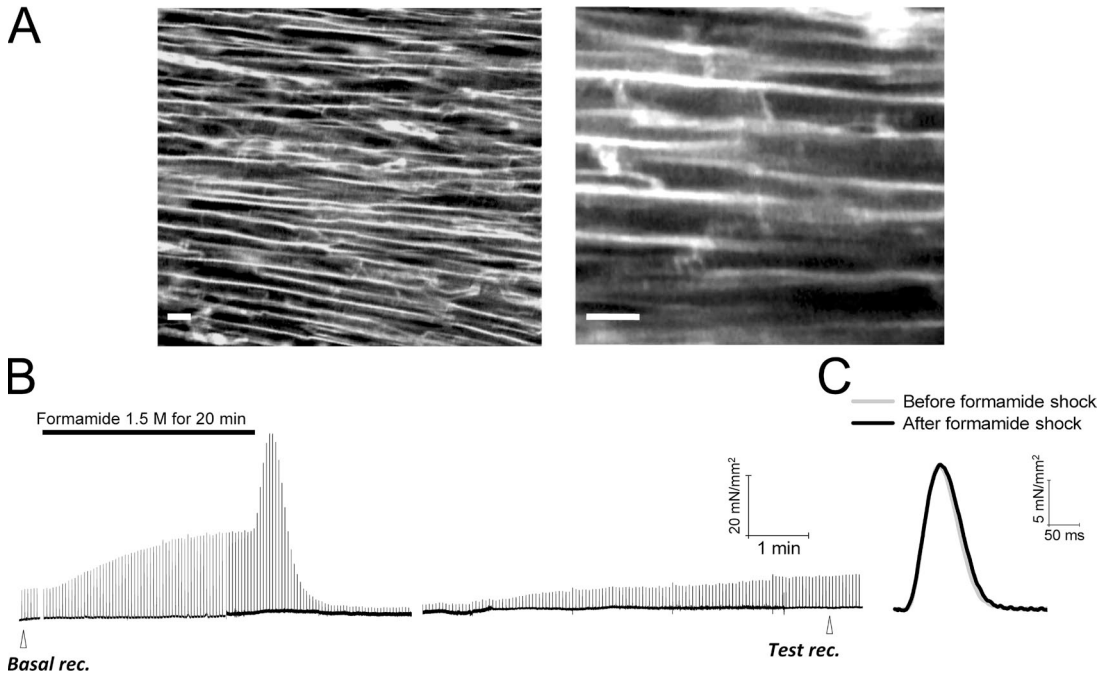

Figure 5. Formamide osmotic shock does not affect mechanical properties of atrial myocardium. (A) TPF images of a rat atrial trabecula loaded with FM4-64. The lack of organized t-tubules is evident. Bars, 10 µm. (B) Transient changes in twitch tension during formamide exposure and washout. Twitch tension shows a significant increase in the presence of formamide, a further enhancement during the initial phase of formamide washout, followed by a rapid decrease below basal levels. All of these changes are comparable to those observed in ventricular trabeculae during formamide treatment. However, in atrial trabeculae, twitch tension recovers basal pre-formamide amplitude and kinetics some minutes after formamide shock. (C) Superimposed representative traces of isometric twitch force at 1-Hz stimulation frequency from an atrial trabecula before and after formamide shock. Extracellular $[Ca^{2+}]_i$ is equal to 1.5 mM.

(e.g., peak time was 91 ± 5 vs. 46 ± 3 ms in detubulated vs. control trabeculae, respectively; $P < 0.01$).

(b) High extracellular [Ca^{2+}] ([Ca^{2+}]$_e$). High $[Ca^{2+}]_o$ (3–10 mmol/L) increases the driving force for Ca^{2+}, leading to enhanced $I_{Ca\text{-}L}$ and increased Ca^{2+} release from the SR (Trafford et al., 2001; Eisner et al., 2013), ultimately increasing twitch amplitude (Redel et al., 2002). Force was recorded during stimulation at 1 Hz in control and detubulated trabeculae exposed to different $[Ca^{2+}]_o$ in the bathing solution, and force parameters were evaluated at steady state. At $[Ca^{2+}]_o = 8$ mmol/L, active stress was not statistically different in detubulated compared with control, but contractions were significantly prolonged (Fig. 6 B).

The observations above indicate that both maximal force generation capacity and maximal Ca^{2+} release ability are maintained after formamide shock, suggesting that detubulation does not alter the function of the contractile machinery nor the ability of the SR to accumulate Ca^{2+}.

Depressed contractile force and slower twitch kinetics of detubulated myocardium can be rescued by enhancing propagation of CICR

The mechanical behavior of detubulated myocardium can be partly attributed to the net decrease of TT currents $I_{Ca\text{-}L}$ and I_{NCX} (Kawai et al., 1999; Brette et al., 2002). The loss of synchronous Ca^{2+} release in the core of detubulated myocytes may further affect contractile

TABLE 2

Atrial trabeculae: Steady-state twitch contractions

Mechanical parameters	Control	Detubulated		Control	Detubulated	
	1 Hz			3 Hz		
Active stress (mN/mm^2)	18.1 ± 5.4	18.6 ± 5.7	NS	21.3 ± 4.6	19.6 ± 3.8	NS
Twitch time to peak (ms)	71 ± 1	73 ± 2	NS	72 ± 2	72 ± 2	NS
Twitch relaxation time 50% (ms)	39 ± 6	42 ± 4	NS	39 ± 6	42 ± 4	NS
Twitch relaxation time 90% (ms)	148 ± 10	151 ± 7	NS	147 ± 10	151 ± 11	NS

Twitch force before and after formamide shock in atrial trabeculae. The time to 50 and 90% relaxation/decay is measured from the peak of the twitch. NS, not significant in paired Student's *t* test. $n = 5$ and 8, number of rats and number of trabeculae, respectively.

function. In areas where t-tubules are lost, orphaned RyR2 clusters can be activated by SR Ca^{2+} release propagation from adjacent regions (Song et al., 2006), albeit with a significant delay. In the experiments reported below, we aimed to test the mechanical effects of Ca^{2+} release resyncronization in detubulated myocardium. Trabeculae were exposed to 200 µmol/L caffeine, which has been used previously at low concentrations (100–500 µmol/L) to increase RyR2 sensitivity (O'Neill and Eisner, 1990; O'Neill et al., 1990; Kong et al., 2008). Force and Ca^{2+} transients were simultaneously measured in the absence and the presence of caffeine at 1 and 3 Hz. In control trabeculae, the increased RyR2 open probability during exposure to 200 µmol/L caffeine led to a transitory increase of Ca^{2+} transient and force amplitude, followed by a mild sustained reduction of both (Fig. 7, A and B). At steady state, the average Ca^{2+} transient decreased by 12 ± 1% and force by 16 ± 2% at a 3-Hz stimulation rate, whereas less pronounced variations were observed at 1 Hz. The decrease of Ca^{2+} transient amplitude was mainly related to an increased diastolic $[Ca^{2+}]_i$, whereas peak systolic $[Ca^{2+}]_i$ remained unchanged. Caffeine slightly prolonged Ca^{2+} transient decay but did not affect twitch kinetics in control trabeculae (Fig. 7, A and B). In detubulated trabeculae instead, caffeine led to a sustained increase of Ca^{2+} transient and twitch amplitude (e.g., average Ca^{2+} transient increased by 15 ± 1% and force by 33 ± 6% at 3 Hz steady state). The caffeine-induced potentiating effect in detubulated trabeculae was more pronounced at the 3-Hz stimulation rate compared with the 1 Hz (Fig. 7 A, inset). Additionally, still at variance with control trabeculae, caffeine significantly hastened Ca^{2+} transient decay and accelerated the kinetics of force development and relaxation in detubulated muscles (Fig. 7 B).

To test whether the positive mechanical effects of 200 µmol/L caffeine in detubulated trabeculae were related to a resynchronization of Ca^{2+} release, we measured CICR transverse propagation velocity in detubulated myocytes in the absence and presence of the drug. Delayed CICR initiation in the cell core was evident in detubulated cardiomyocytes, whereas in control myocytes, Ca^{2+} release was always synchronous through the entire cell thickness (Fig. 8 A). As shown in Fig. 8 B, caffeine caused a 2.3-fold increase of CICR transverse propagation velocity in detubulated myocytes. Increased RyR2 Ca sensitivity by caffeine reduced the delay between surface and cell core activation, thereby likely improving the timing and extent of myofibril recruitment in detubulated areas.

DISCUSSION

Successful detubulation of ventricular trabeculae

The results of this study validate a method to induce detubulation in intact ventricular muscle using formamide-induced osmotic shock. Formamide shock has been used previously to detach t-tubules in isolated adult rat

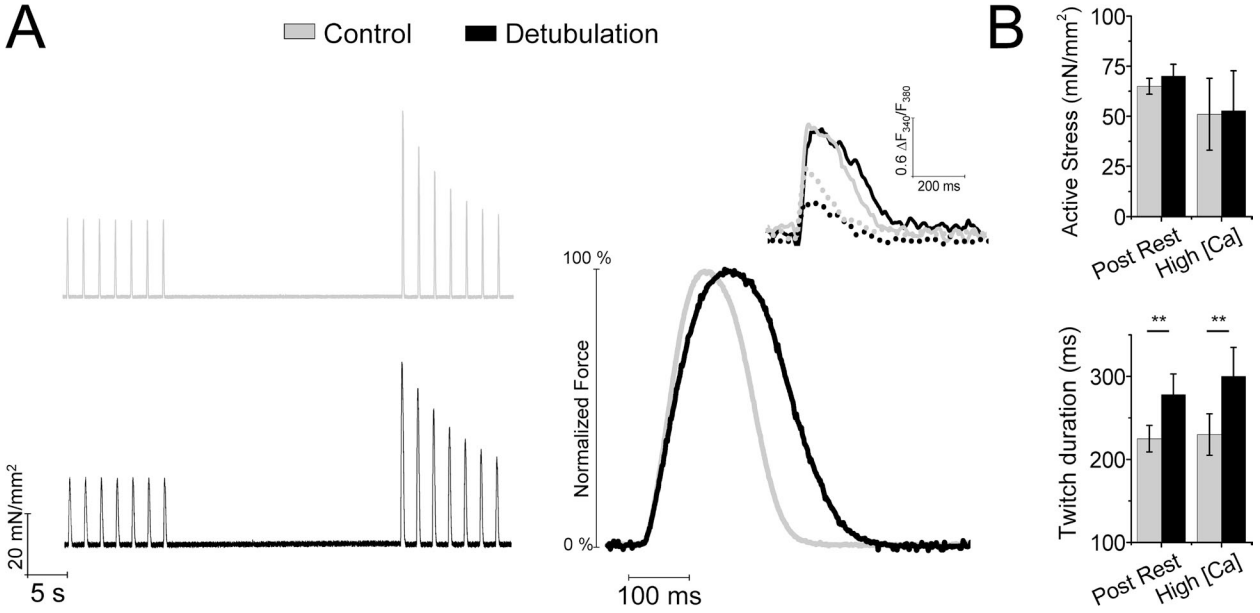

Figure 6. Effects of acute detubulation on maximal twitch force in post-rest potentiated beats and high extracellular $[Ca^{2+}]$. (A) Representative traces of isometric twitch force after 30-s stimulation pauses in a trabecula before and after formamide treatment. (Inset) Superimposed Ca^{2+} transients at baseline (0.5 Hz; dotted lines) and after pauses (continuous lines) before and after detubulation (black and gray, respectively). (B) Mean ± SE data of twitch tension and kinetics after 30-s pauses (Post Rest) and at 8 mM of extracellular $[Ca^{2+}]$ (High [Ca]). **, $P < 0.01$, paired. $n = 10$ and 13, number of rats and number of trabeculae, respectively.

ventricular myocytes (Kawai et al., 1999; Brette et al., 2002). Detachment of t-tubules from the sarcolemma upon formamide shock is thought to occur when myocytes swell rapidly (<1 min) and modestly (15–20%) upon withdrawal of the highly permeant formamide (Kawai et al., 1999; Brette et al., 2002). In agreement with these findings, thin trabeculae (width of <200 µm) that show detubulation exhibit rapid (<30 s) swelling (~17% volume increase) upon formamide washout with complete solution exchange occurring within 10 s. The success of the present study explains why previous efforts to detubulate intact cardiac muscle failed (Chapman, 1980): the preparations used were large (>400 µm) papillary muscles, and the detubulation agent was glycerol, which diffuses more slowly than formamide across lipid bilayers, preventing fast and reversible volume changes.

Experiments with membrane-selective fluorescent dyes and TPF imaging strongly support the conclusion that a fraction of t-tubules is detached from the surface membrane after formamide shock (Fig. 2), and that disconnected t-tubules remain "trapped" within the myocytes. T-tubule detachment was also confirmed by directly probing the electrical function of TT membranes using the RAMP microscope and voltage-sensitive dyes: formamide shock led to the absence of action potentials in most of the t-tubules, despite the fact that electrical activity at the surface sarcolemma was maintained (Fig. 2). In detubulated trabeculae, we also found a shorter action potential duration at 50 and 90% repolarization, which is in agreement with previous data on single cardiomyocytes and underlies a loss of TT L-type Ca^{2+} current.

Detubulation of trabeculae was usually incomplete, as indicated by the large intracellular and intercellular variability of cross-striation density after formamide shock (Fig. 2). This result may be inherent to the formamide shock method because variable degrees of detubulation were also noted in single isolated cardiomyocytes subjected to the formamide shock (Smyrnias et al., 2010; Sacconi et al., 2012). Far from representing a hindrance

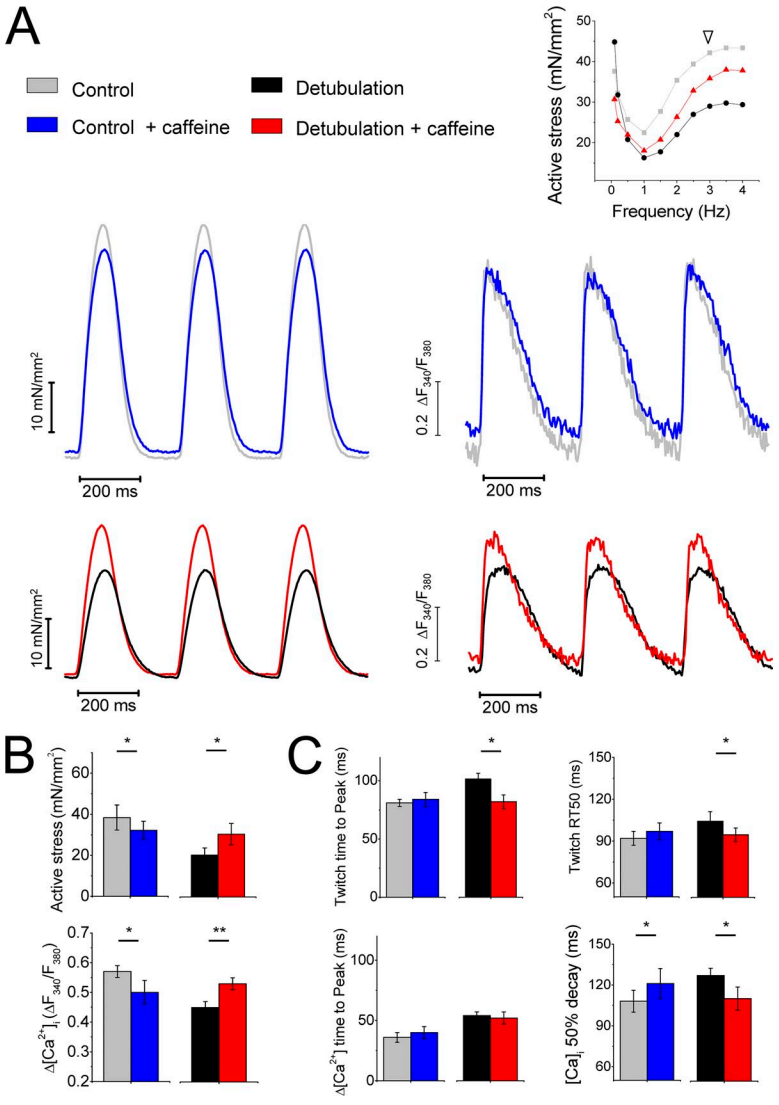

Figure 7. Low-dose caffeine selectively improves twitch force and contractile kinetics in detubulated trabeculae. (A) Representative traces showing steady-state twitches at 3 Hz (left) and corresponding $[Ca^{2+}]_i$ transients (right) in a rat trabecula before and after formamide shock, at baseline (gray and black) and in the presence of 200 µmol/L caffeine (blue and red). (Inset) Force–frequency relationship in the same muscle showing that the effect of caffeine on twitch tension after detubulation was more prominent at a high frequency. (B) Twitch and $[Ca^{2+}]_i$ amplitude at baseline and in the presence of 200 µmol/L caffeine. (C) Twitch kinetics and $[Ca^{2+}]_i$ transient kinetics at baseline and in the presence of 200 µmol/L caffeine. Means ± SE from seven rat ventricular trabeculae (four rats). *, $P < 0.05$; **, $P < 0.01$, paired, caffeine versus baseline.

of the present model, the incomplete and variable detubulation more closely resembles pathological conditions, where complete TT loss is rarely observed. In fact, in all disease settings including atrial fibrillation, ischemic heart failure, and genetic cardiomyopathies (He et al., 2001; Louch et al., 2004; Heinzel et al., 2008; Lenaerts et al., 2009; Lyon et al., 2009), myocyte detubulation is always described as a partial loss of TT structures with overt disorganization of the TT network and clear variability among cells.

We found no decrease in force and no alteration of contraction kinetics in formamide-treated atrial trabeculae (Fig. 5 and Table 2). This observation rules out the possibility that the mechanical changes occurring in formamide-detubulated ventricular trabeculae are caused by damage to cell structures other than t-tubules.

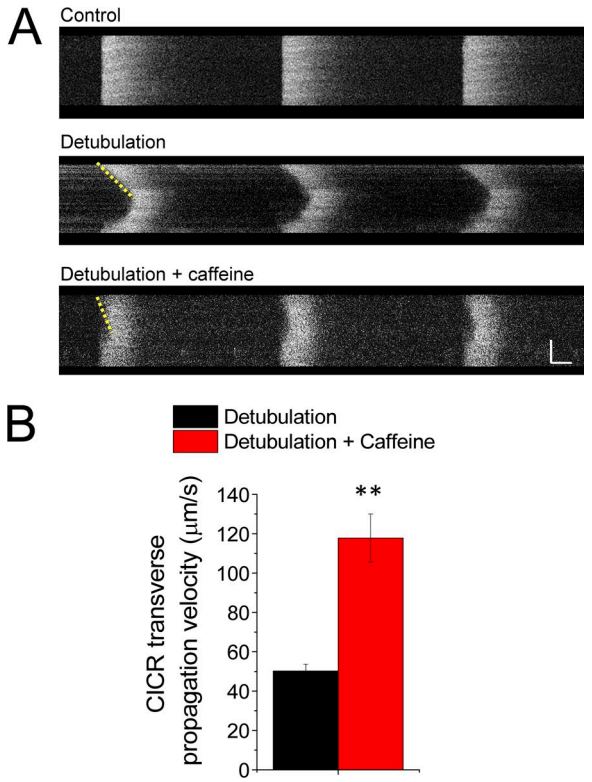

Figure 8. Low-dose caffeine improves CICR transverse propagation velocity in detubulated myocytes. (A) Representative confocal line scan images of Fluoforte-loaded cardiomyocytes showing steady-state Ca^{2+} transients at 1 Hz, 1 mM $[Ca^{2+}]_o$, and room temperature. (B) Mean data of CICR transverse propagation velocity in detubulated myocytes in the absence and presence of 200 µM caffeine. Velocity was taken from the slope of the Ca^{2+} wave in line scan images (dotted lines in yellow). Data are mean ± SE. The XY scale bar is 100 ms × 10 µm. **, $P < 0.01$, unpaired. The total number of myocytes tested was: 40 in the control group, 71 in the detubulated group, and 54 in the detubulated plus caffeine group. Myocytes were isolated from four rat hearts.

Mechanisms of myocardial dysfunction in detubulated muscle

Acute detubulation reduces steady-state twitch force, impairs positive inotropic response to high stimulation frequencies, and slows the kinetics of force generation and relaxation. Simultaneous recording of force and Ca^{2+} transients in trabeculae allowed us to ascertain that all twitch force changes occurring after formamide shock can be explained by related alterations of intracellular Ca^{2+} cycling.

Previous work on detubulated single ventricular cardiomyocytes (Yang et al., 2002; Brette et al., 2004; Orchard et al., 2009) highlighted the loss of TT proteins as a primary determinant of the altered Ca^{2+} cycling. Because 80% of $I_{Ca\text{-}L}$ and 63% of NCX activity are located in the TT membranes (Yang et al., 2002; Pásek et al., 2008; Chase et al., 2010), even a partial disconnection of t-tubules would lead to a reduction of these currents. A decrease in the amplitude of $I_{Ca\text{-}L}$ (Kawai et al., 1999; Brette et al., 2002) and the corresponding significant reduction of the overall cytosolic Ca^{2+} transient is consistent with the reduced twitch force observed under basal conditions in detubulated ventricular trabeculae. Additionally, a partial loss of TT $I_{Ca\text{-}L}$ contributes to the reduced positive force–frequency response (Fowler et al., 2004) because of a reduction of Ca^{2+} influx per unit of time ("Ca^{2+} gain") in detubulated muscles (Schouten and ter Keurs, 1991).

The loss of operational NCX, as confirmed by the ∼17% increase of Ca^{2+} recirculation fraction that we observed in detubulated trabeculae (Ferrantini et al., 2010), may explain the slower kinetics of the late phase of relaxation in detubulated myocardium. Consistently, previous work has shown that NCX blockers prolong the decay of intracellular Ca^{2+} transients and relaxation time of unloaded single myocytes (Ozdemir et al., 2008), with the contribution of NCX to $[Ca^{2+}]_i$ decline being most apparent during the terminal phase of relaxation (Yao et al., 1997). In healthy myocytes, increase in the number of action potentials per time unit causes cytosolic accumulation of Na^+ that may enhance reverse-mode NCX activity, thus contributing to increase Ca^{2+} entry at high pacing rates (Ozdemir et al., 2008); this mechanism ("Na^+ gain") is partially lost in detubulated myocardium. Thus, in terms of contractile force, loss of operational NCX may concur with reduction of I_{CaL} to the blunted positive inotropic effect of high pacing rates. However, because NCX is a main mode of Ca extrusion from cardiac myocytes, the loss of TT NCX will limit Ca^{2+} extrusion and may allow relatively normal SR Ca^{2+} content, despite the reduced I_{CaL}. Preserved SR Ca^{2+} content in detubulated cardiomyocytes has indeed been experimentally confirmed (Brette et al., 2005).

The partial loss of $I_{Ca\text{-}L}$ and NCX contributes to most of the functional consequences of acute detubulation.

However, the prolongation of the kinetics of Ca^{2+} transient rise and of twitch force generation can hardly be a direct consequence of the loss of $I_{Ca\text{-}L}$ and NCX and thus requires a different explanation.

Propagated CICR after detubulation

In agreement with previous work (Brette et al., 2005), we showed that in acutely detubulated ventricular myocytes, Ca^{2+} transients begin with a fast rise in the subsarcolemmal area, followed by a variable degree of Ca^{2+} release that propagates toward the cell core. RyR2 open probability, SR Ca^{2+} content, and sarcolemmal Ca^{2+} entry interplay to determine the extent and velocity of transverse CICR propagation (Brette et al., 2005). Here, we observed that twitch tension of detubulated trabeculae is normalized in post-rest beats or high extracellular [Ca^{2+}], although contraction kinetics is still prolonged. Additionally, we tested the effects of caffeine as a RyR2 Ca^{2+}-sensitizing agent. 200µmol/L caffeine showed the following effects: (a) a significant increase of transverse CICR propagation velocity in detubulated cardiomyocytes, and (b) a partial restoration of twitch amplitude and kinetics as well as Ca^{2+} transient kinetics (including peak time and 50% relaxation) in detubulated trabeculae. Previous evidence support the hypothesis that increased RyR2 open probability (either pharmacologically determined or induced by genetic mutations) enhances Ca^{2+} release propagation velocity (Xiao et al., 2007; Liu et al., 2013); conversely, RyR2-desensitizing interventions (JTV-519, flecainide) slow the velocity of Ca^{2+} wave propagation (Loughrey et al., 2007; Galimberti and Knollmann, 2011). The reliance of the detubulated myocytes on transversely propagated CICR renders activation of Ca^{2+} release more dependent on RyR2 gating properties and refractoriness, which in turn tightly depends on the interval between beats.

The velocity and extent of CICR propagation may decrease at high stimulation frequency because of accumulating RyR2 refractoriness (Maier et al., 2000). This could be an additional factor limiting the positive force–frequency response in detubulated myocardium, in addition to the reduced Ca^{2+} and Na^{+} gain per time unit, as described above. In line with this idea, the increase in twitch tension induced by caffeine was more prominent at 3 than at 1 Hz (Fig. 7). On the other hand, low pacing rates and long stimulation pauses may be especially beneficial for improving transverse CICR propagation, because RyR2 channels are fully recovered from inactivation/adaptation. Consistently, we showed that detubulated trabeculae get the most benefit from the prolonged diastolic period at low rates (Fig. 4) or after long pauses (Fig. 6), with twitch tension rising up to control levels.

Furthermore, in detubulated myocardium, reduced action potential duration (Fig. 3) may contribute to reduce integrated Ca^{2+} current and thus diminish net Ca^{2+} entry and SR Ca^{2+} content. That by itself would worsen transverse CICR propagation, reducing the amplitude of global Ca^{2+} transients. In high extracellular calcium (e.g., 8 mM), potentiation of sarcolemmal Ca^{2+} trigger and SR content, together with RyR2 Ca^{2+} sensitization (by cytosolic Ca^{2+} accumulation), can positively affect CICR transverse propagation, thus enhancing myofibril recruitment and contractile force.

However, Ca^{2+} transients and twitches were still markedly prolonged in post-rest contractions and high extracellular calcium. Conversely, restoration of RyR2 sensitivity with caffeine in detubulated regions accelerates twitch kinetics (in addition to the positive inotropic effect). Such a remarkable effect of a low dose of caffeine in detubulated trabeculae may be related to the depressed Ca^{2+} sensitivity of those RyR2 channels that are structurally or functionally uncoupled from t-tubules, as suggested by previous studies in cardiomyocytes (Brette et al., 2005). A low dose of caffeine may thus be more effective than other interventions because it directly increases the intrinsically depressed RyR2 Ca^{2+} sensitivity of detubulated myocytes. In rodent atrial cardiomyocytes, which have specialized SR structures (Z-tubules) to facilitate CICR transverse propagation, 200 µM caffeine almost fully normalized Ca^{2+} transient amplitude and kinetics (Mackenzie et al., 2004). In acutely detubulated ventricular myocardium, with no SR structures that are specialized to compensate for the absence of t-tubules, the caffeine-normalizing effect is only partial and may be tightly correlated to the degree of TT detachment.

In chronically detubulated diseased cardiomyocytes, CICR propagation occurs from areas with remaining functional t-tubules to those devoid of t-tubules (Louch et al., 2004, 2006, 2010; Heinzel et al., 2008) or to areas where t-tubules are electrically uncoupled from the surface (Sacconi et al., 2012). Synchronization of Ca^{2+} release by low-dose caffeine has been described already in a model of chronic detubulation (Øyehaug et al., 2013). Formamide-treated trabeculae resemble diseased myocardial tissue, in that the degree of TT disruption is variable among neighboring myocytes (He et al., 2001; Louch et al., 2004; Heinzel et al., 2008; Lenaerts et al., 2009; Lyon et al., 2009). The coexistence of myocytes with partial and asynchronous activation in series with myocytes with synchronous and complete activation of all myofibril layers may by itself decrease the uniformity of muscle contraction, thus reducing developed force and affecting the kinetics of force development and relaxation. Our data suggest that, in detubulated myocardium, any intervention aimed at normalizing the depressed open probability of the orphaned RyR2 clusters could be beneficial in enhancing tension and resynchronizing contraction.

Mechanical changes after detubulation: Implications for cardiac disease and therapy

Mechanical changes occurring as a consequence of detubulation may be relevant for cardiac diseases associated

with reduced TT density (He et al., 2001; Louch et al., 2004; Heinzel et al., 2008; Lenaerts et al., 2009; Lyon et al., 2009), in which detubulation may contribute to both systolic and diastolic dysfunction. For instance, in CHF, reduced force and slower relaxation are the results of complex changes in sarcolemma, SR, and myofilament function. Reduction in the density of functional t-tubules can further weaken (and prolong) contraction, contributing to systolic dysfunction and blunted force–frequency response, which is a hallmark of CHF (Niu et al., 2007). Work based on animal studies led to the assumption that TT disruption is a major detriment to cardiac output in human disease. However, massive TT disruption also occurs in genetic heart diseases such as hypertrophic cardiomyopathy (Lyon et al., 2009), which is characterized by slower kinetics of Ca^{2+} transients and myocardial contraction, leading to diastolic dysfunction in the absence of primary systolic impairment (Olivotto et al., 2012; Coppini et al., 2013). We showed that twitch amplitude is not reduced by detubulation at low pacing rates, suggesting that transverse CICR propagation may compensate more effectively for T-tubule loss in larger mammals, where the heart rate is lower. On the other hand, delayed initiation and prolongation of relaxation caused by loss of t-tubules may contribute to impair myocardial relaxation and thus be a significant determinant of diastolic (rather than systolic) dysfunction in hypertrophic cardiomyopathy and other cardiac conditions in patients. In addition to the mechanical effects, nonuniform excitation–contraction coupling could in turn promote initiation of propagated calcium waves and arrhythmias, especially under conditions of SR Ca^{2+} overload. This mechanism may be relevant for disease: myocardial ischemia can lead to an acute form of detubulation in the infarct border zone (Louch et al., 2006), where nonuniformity of contraction may contribute to the increased probability of arrhythmias (ter Keurs et al., 2006).

Detubulation leads to a shift from synchronous SR Ca^{2+} release throughout the entire myocyte to propagated CICR. In this condition, Ca^{2+} release starts where TATS and SR are coupled and propagates to areas lacking TT with significant delay, diminishing the efficacy in recruiting deep myofibril layers. However, propagated CICR mode may open new possibilities for therapeutic approaches, aimed at improving contractile force by enhancing propagation of SR Ca^{2+} release to recruit all myofibril layers. The positive effects of RyR2 sensitization with caffeine is shown here as a proof of concept, but its pro-arrhythmic potential excludes any possible therapeutic application in cardiac disease.

We thank Ping Yan and Leslie M. Loew for providing the Di-4-AN(F)EPPTEA voltage-sensitive dye.

This work was supported by the EU (STREP project 241577 "BIG HEART," seventh European Framework Program, to C. Poggesi), the Telethon (grant GGP13162), and the Heart and Stroke Foundations of Alberta, the North West Territories and Nunavut.

The authors declare no competing financial interests.

Richard L. Moss served as editor.

Submitted: 22 October 2013
Accepted: 9 May 2014

REFERENCES

Allegra Mascaro, A.L., L. Sacconi, and F.S. Pavone. 2010. Multiphoton nanosurgery in live brain. *Front Neuroenergetics.* 2:21.

Bassani, R.A., and D.M. Bers. 1994. Na-Ca exchange is required for rest-decay but not for rest-potentiation of twitches in rabbit and rat ventricular myocytes. *J. Mol. Cell. Cardiol.* 26:1335–1347. http://dx.doi.org/10.1006/jmcc.1994.1152

Baudino, T.A., W. Carver, W. Giles, and T.K. Borg. 2006. Cardiac fibroblasts: friend or foe? *Am. J. Physiol. Heart Circ. Physiol.* 291:H1015–H1026. http://dx.doi.org/10.1152/ajpheart.00023.2006

Bers, D.M., R.A. Bassani, J.W. Bassani, S. Baudet, and L.V. Hryshko. 1993. Paradoxical twitch potentiation after rest in cardiac muscle: Increased fractional release of SR calcium. *J. Mol. Cell. Cardiol.* 25:1047–1057. http://dx.doi.org/10.1006/jmcc.1993.1117

Brette, F., K. Komukai, and C.H. Orchard. 2002. Validation of formamide as a detubulation agent in isolated rat cardiac cells. *Am. J. Physiol. Heart Circ. Physiol.* 283:H1720–H1728.

Brette, F., L. Sallé, and C.H. Orchard. 2004. Differential modulation of L-type Ca^{2+} current by SR Ca^{2+} release at the T-tubules and surface membrane of rat ventricular myocytes. *Circ. Res.* 95:e1–e7. http://dx.doi.org/10.1161/01.RES.0000135547.53927.F6

Brette, F., S. Despa, D.M. Bers, and C.H. Orchard. 2005. Spatiotemporal characteristics of SR Ca^{2+} uptake and release in detubulated rat ventricular myocytes. *J. Mol. Cell. Cardiol.* 39:804–812. http://dx.doi.org/10.1016/j.yjmcc.2005.08.005

Chapman, R.A. 1980. Excitation-contraction coupling in cardiac muscle. *Prog. Biophys. Mol. Biol.* 35:1–52. http://dx.doi.org/10.1016/0079-6107(80)90002-4

Chase, A., J. Colyer, and C.H. Orchard. 2010. Localised Ca channel phosphorylation modulates the distribution of L-type Ca current in cardiac myocytes. *J. Mol. Cell. Cardiol.* 49:121–131. http://dx.doi.org/10.1016/j.yjmcc.2010.02.017

Cicchi, R., L. Sacconi, A. Jasaitis, R.P. O'Connor, D. Massi, S. Sestini, V. De Giorgi, T. Lotti, and F.S. Pavone. 2008. Multidimensional custom-made non-linear microscope: from ex-vivo to in-vivo imaging. *Appl. Phys. B.* 92:359–365. http://dx.doi.org/10.1007/s00340-008-3130-3

Coppini, R., C. Ferrantini, L. Yao, P. Fan, M. Del Lungo, F. Stillitano, L. Sartiani, B. Tosi, S. Suffredini, C. Tesi, et al. 2013. Late sodium current inhibition reverses electromechanical dysfunction in human hypertrophic cardiomyopathy. *Circulation.* 127:575–584. http://dx.doi.org/10.1161/CIRCULATIONAHA.112.134932

de Tombe, P.P., and H.E. ter Keurs. 1990. Force and velocity of sarcomere shortening in trabeculae from rat heart. Effects of temperature. *Circ. Res.* 66:1239–1254. http://dx.doi.org/10.1161/01.RES.66.5.1239

Dibb, K.M., J.D. Clarke, M.A. Horn, M.A. Richards, H.K. Graham, D.A. Eisner, and A.W. Trafford. 2009. Characterization of an extensive transverse tubular network in sheep atrial myocytes and its depletion in heart failure. *Circ Heart Fail.* 2:482–489. http://dx.doi.org/10.1161/CIRCHEARTFAILURE.109.852228

Eisner, D., E. Bode, L. Venetucci, and A. Trafford. 2013. Calcium flux balance in the heart. *J. Mol. Cell. Cardiol.* 58:110–117. http://dx.doi.org/10.1016/j.yjmcc.2012.11.017

Ferrantini, C., R. Coppini, G.L. Wang, M.L. Zhang, E. de Vries, C. Tesi, C. Poggesi, and H.T. Keurs. 2010. Impact of loss of T-tubules on myocardial contractile force and kinetics. *Biophys. J.* 98:5a. http://dx.doi.org/10.1016/j.bpj.2009.12.035

Ferrantini, C., C. Crocini, R. Coppini, F. Vanzi, C. Tesi, E. Cerbai, C. Poggesi, F.S. Pavone, and L. Sacconi. 2013. The transverse-axial tubular system of cardiomyocytes. *Cell. Mol. Life Sci.* 70:4695–4710. http://dx.doi.org/10.1007/s00018-013-1410-5

Fowler, M.R., R.S. Dobson, C.H. Orchard, and S.M. Harrison. 2004. Functional consequences of detubulation of isolated rat ventricular myocytes. *Cardiovasc. Res.* 62:529–537. http://dx.doi.org/10.1016/j.cardiores.2004.02.008

Galimberti, E.S., and B.C. Knollmann. 2011. Efficacy and potency of class I antiarrhythmic drugs for suppression of Ca^{2+} waves in permeabilized myocytes lacking calsequestrin. *J. Mol. Cell. Cardiol.* 51:760–768. http://dx.doi.org/10.1016/j.yjmcc.2011.07.002

Hanley, P.J., A.A. Young, I.J. LeGrice, S.G. Edgar, and D.S. Loiselle. 1999. 3-Dimensional configuration of perimysial collagen fibres in rat cardiac muscle at resting and extended sarcomere lengths. *J. Physiol.* 517:831–837. http://dx.doi.org/10.1111/j.1469-7793.1999.0831s.x

Hasenfuss, G., W. Schillinger, S.E. Lehnart, M. Preuss, B. Pieske, L.S. Maier, J. Prestle, K. Minami, and H. Just. 1999. Relationship between Na^+-Ca^{2+}-exchanger protein levels and diastolic function of failing human myocardium. *Circulation.* 99:641–648. http://dx.doi.org/10.1161/01.CIR.99.5.641

He, J., M.W. Conklin, J.D. Foell, M.R. Wolff, R.A. Haworth, R. Coronado, and T.J. Kamp. 2001. Reduction in density of transverse tubules and L-type Ca^{2+} channels in canine tachycardia-induced heart failure. *Cardiovasc. Res.* 49:298–307. http://dx.doi.org/10.1016/S0008-6363(00)00256-X

Heinzel, F.R., V. Bito, L. Biesmans, M. Wu, E. Detre, F. von Wegner, P. Claus, S. Dymarkowski, F. Maes, J. Bogaert, et al. 2008. Remodeling of T-tubules and reduced synchrony of Ca^{2+} release in myocytes from chronically ischemic myocardium. *Circ. Res.* 102:338–346. http://dx.doi.org/10.1161/CIRCRESAHA.107.160085

Kawai, M., M. Hussain, and C.H. Orchard. 1999. Excitation-contraction coupling in rat ventricular myocytes after formamide-induced detubulation. *Am. J. Physiol.* 277:H603–H609.

Kong, H., P.P. Jones, A. Koop, L. Zhang, H.J. Duff, and S.R. Chen. 2008. Caffeine induces Ca^{2+} release by reducing the threshold for luminal Ca^{2+} activation of the ryanodine receptor. *Biochem. J.* 414:441–452. http://dx.doi.org/10.1042/BJ20080489

Lamberts, R.R., N. Hamdani, T.W. Soekhoe, N.M. Boontje, R. Zaremba, L.A. Walker, P.P. de Tombe, J. van der Velden, and G.J. Stienen. 2007. Frequency-dependent myofilament Ca^{2+} desensitization in failing rat myocardium. *J. Physiol.* 582:695–709. http://dx.doi.org/10.1113/jphysiol.2007.134486

Lenaerts, I., V. Bito, F.R. Heinzel, R.B. Driesen, P. Holemans, J. D'hooge, H. Heidbüchel, K.R. Sipido, and R. Willems. 2009. Ultrastructural and functional remodeling of the coupling between Ca^{2+} influx and sarcoplasmic reticulum Ca^{2+} release in right atrial myocytes from experimental persistent atrial fibrillation. *Circ. Res.* 105:876–885. http://dx.doi.org/10.1161/CIRCRESAHA.109.206276

Liu, N., M. Denegri, W. Dun, S. Boncompagni, F. Lodola, F. Protasi, C. Napolitano, P.A. Boyden, and S.G. Priori. 2013. Abnormal propagation of calcium waves and ultrastructural remodeling in recessive catecholaminergic polymorphic ventricular tachycardia. *Circ. Res.* 113:142–152. http://dx.doi.org/10.1161/CIRCRESAHA.113.301783

Louch, W.E., V. Bito, F.R. Heinzel, R. Macianskiene, J. Vanhaecke, W. Flameng, K. Mubagwa, and K.R. Sipido. 2004. Reduced synchrony of Ca^{2+} release with loss of T-tubules–a comparison to Ca^{2+} release in human failing cardiomyocytes. *Cardiovasc. Res.* 62:63–73. http://dx.doi.org/10.1016/j.cardiores.2003.12.031

Louch, W.E., H.K. Mørk, J. Sexton, T.A. Strømme, P. Laake, I. Sjaastad, and O.M. Sejersted. 2006. T-tubule disorganization and reduced synchrony of Ca^{2+} release in murine cardiomyocytes following myocardial infarction. *J. Physiol.* 574:519–533. http://dx.doi.org/10.1113/jphysiol.2006.107227

Louch, W.E., O.M. Sejersted, and F. Swift. 2010. There goes the neighborhood: Pathological alterations in T-tubule morphology and consequences for cardiomyocyte Ca^{2+} handling. *J. Biomed. Biotechnol.* 2010:503906. http://dx.doi.org/10.1155/2010/503906

Loughrey, C.M., N. Otani, T. Seidler, M.A. Craig, R. Matsuda, N. Kaneko, and G.L. Smith. 2007. K201 modulates excitation-contraction coupling and spontaneous Ca^{2+} release in normal adult rabbit ventricular cardiomyocytes. *Cardiovasc. Res.* 76:236–246. http://dx.doi.org/10.1016/j.cardiores.2007.06.014

Lyon, A.R., K.T. MacLeod, Y. Zhang, E. Garcia, G.K. Kanda, M.J. Lab, Y.E. Korchev, S.E. Harding, and J. Gorelik. 2009. Loss of T-tubules and other changes to surface topography in ventricular myocytes from failing human and rat heart. *Proc. Natl. Acad. Sci. USA.* 106:6854–6859. http://dx.doi.org/10.1073/pnas.0809777106

Mackenzie, L., H.L. Roderick, M.J. Berridge, S.J. Conway, and M.D. Bootman. 2004. The spatial pattern of atrial cardiomyocyte calcium signalling modulates contraction. *J. Cell Sci.* 117:6327–6337. http://dx.doi.org/10.1242/jcs.01559

Maier, L.S., D.M. Bers, and B. Pieske. 2000. Differences in Ca^{2+}-handling and sarcoplasmic reticulum Ca^{2+}-content in isolated rat and rabbit myocardium. *J. Mol. Cell. Cardiol.* 32:2249–2258. http://dx.doi.org/10.1006/jmcc.2000.1252

Niu, C.F., Y. Watanabe, K. Ono, T. Iwamoto, K. Yamashita, H. Satoh, T. Urushida, H. Hayashi, and J. Kimura. 2007. Characterization of SN-6, a novel Na^+/Ca^{2+} exchange inhibitor in guinea pig cardiac ventricular myocytes. *Eur. J. Pharmacol.* 573:161–169. http://dx.doi.org/10.1016/j.ejphar.2007.06.033

O'Neill, S.C., and D.A. Eisner. 1990. A mechanism for the effects of caffeine on Ca^{2+} release during diastole and systole in isolated rat ventricular myocytes. *J. Physiol.* 430:519–536.

O'Neill, S.C., P. Donoso, and D.A. Eisner. 1990. The role of $[Ca^{2+}]_i$ and $[Ca^{2+}]$ sensitization in the caffeine contracture of rat myocytes: Measurement of $[Ca^{2+}]_i$ and $[caffeine]_i$. *J. Physiol.* 425:55–70.

Olivotto, I., F. Cecchi, C. Poggesi, and M.H. Yacoub. 2012. Patterns of disease progression in hypertrophic cardiomyopathy: An individualized approach to clinical staging. *Circ Heart Fail.* 5:535–546. http://dx.doi.org/10.1161/CIRCHEARTFAILURE.112.967026

Orchard, C.H., M. Pásek, and F. Brette. 2009. The role of mammalian cardiac t-tubules in excitation-contraction coupling: experimental and computational approaches. *Exp. Physiol.* 94:509–519. http://dx.doi.org/10.1113/expphysiol.2008.043984

Øyehaug, L., K.O. Loose, G.F. Jølle, A.T. Røe, I. Sjaastad, G. Christensen, O.M. Sejersted, and W.E. Louch. 2013. Synchrony of cardiomyocyte Ca^{2+} release is controlled by T-tubule organization, SR Ca^{2+} content, and ryanodine receptor Ca^{2+} sensitivity. *Biophys. J.* 104:1685–1697. http://dx.doi.org/10.1016/j.bpj.2013.03.022

Ozdemir, S., V. Bito, P. Holemans, L. Vinet, J.J. Mercadier, A. Varro, and K.R. Sipido. 2008. Pharmacological inhibition of na/ca exchange results in increased cellular Ca^{2+} load attributable to the predominance of forward mode block. *Circ. Res.* 102:1398–1405. http://dx.doi.org/10.1161/CIRCRESAHA.108.173922

Pásek, M., F. Brette, A. Nelson, C. Pearce, A. Qaiser, G. Christe, and C.H. Orchard. 2008. Quantification of t-tubule area and protein distribution in rat cardiac ventricular myocytes. *Prog. Biophys. Mol. Biol.* 96:244–257. http://dx.doi.org/10.1016/j.pbiomolbio.2007.07.016

Redel, A., W. Baumgartner, K. Golenhofen, D. Drenckhahn, and N. Golenhofen. 2002. Mechanical activity and force–frequency relationship of isolated mouse papillary muscle: effects of extracellular calcium concentration, temperature and contraction type. *Pflugers Arch.* 445:297–304. http://dx.doi.org/10.1007/s00424-002-0931-9

Sacconi, L., C. Ferrantini, J. Lotti, R. Coppini, P. Yan, L.M. Loew, C. Tesi, E. Cerbai, C. Poggesi, and F.S. Pavone. 2012. Action potential propagation in transverse-axial tubular system is impaired in

heart failure. *Proc. Natl. Acad. Sci. USA.* 109:5815–5819. http://dx.doi.org/10.1073/pnas.1120188109

Schouten, V.J., and H.E. ter Keurs. 1991. Role of i_{ca} and Na^+/Ca^{2+} exchange in the force-frequency relationship of rat heart muscle. *J. Mol. Cell. Cardiol.* 23:1039–1050. http://dx.doi.org/10.1016/0022-2828(91)91639-9

Smyrnias, I., W. Mair, D. Harzheim, S.A. Walker, H.L. Roderick, and M.D. Bootman. 2010. Comparison of the T-tubule system in adult rat ventricular and atrial myocytes, and its role in excitation-contraction coupling and inotropic stimulation. *Cell Calcium.* 47:210–223. http://dx.doi.org/10.1016/j.ceca.2009.10.001

Song, L.S., E.A. Sobie, S. McCulle, W.J. Lederer, C.W. Balke, and H. Cheng. 2006. Orphaned ryanodine receptors in the failing heart. *Proc. Natl. Acad. Sci. USA.* 103:4305–4310. http://dx.doi.org/10.1073/pnas.0509324103

ter Keurs, H.E., Y. Wakayama, M. Miura, T. Shinozaki, B.D. Stuyvers, P.A. Boyden, and A. Landesberg. 2006. Arrhythmogenic Ca^{2+} release from cardiac myofilaments. *Prog. Biophys. Mol. Biol.* 90:151–171. http://dx.doi.org/10.1016/j.pbiomolbio.2005.07.002

Trafford, A.W., M.E. Díaz, and D.A. Eisner. 2001. Coordinated control of cell Ca^{2+} loading and triggered release from the sarcoplasmic reticulum underlies the rapid inotropic response to increased L-type Ca^{2+} current. *Circ. Res.* 88:195–201. http://dx.doi.org/10.1161/01.RES.88.2.195

Ward, M.L., D.J. Crossman, and M.B. Cannell. 2011. Mechanisms of reduced contractility in an animal model of hypertensive heart failure. *Clin. Exp. Pharmacol. Physiol.* 38:711–716. http://dx.doi.org/10.1111/j.1440-1681.2011.05563.x

Xiao, B., X. Tian, W. Xie, P.P. Jones, S. Cai, X. Wang, D. Jiang, H. Kong, L. Zhang, K. Chen, et al. 2007. Functional consequence of protein kinase A-dependent phosphorylation of the cardiac ryanodine receptor: Sensitization of store overload-induced Ca^{2+} release. *J. Biol. Chem.* 282:30256–30264. http://dx.doi.org/10.1074/jbc.M703510200

Yan, P., C.D. Acker, W.L. Zhou, P. Lee, C. Bollensdorff, A. Negrean, J. Lotti, L. Sacconi, S.D. Antic, P. Kohl, et al. 2012. Palette of fluorinated voltage-sensitive hemicyanine dyes. *Proc. Natl. Acad. Sci. USA.* 109:20443–20448. http://dx.doi.org/10.1073/pnas.1214850109

Yang, Z., C. Pascarel, D.S. Steele, K. Komukai, F. Brette, and C.H. Orchard. 2002. Na^+-Ca^{2+} exchange activity is localized in the T-tubules of rat ventricular myocytes. *Circ. Res.* 91:315–322. http://dx.doi.org/10.1161/01.RES.0000030180.06028.23

Yano, M., Y. Ikeda, and M. Matsuzaki. 2005. Altered intracellular Ca^{2+} handling in heart failure. *J. Clin. Invest.* 115:556–564. http://dx.doi.org/10.1172/JCI24159

Yao, A., H. Matsui, K.W. Spitzer, J.H. Bridge, and W.H. Barry. 1997. Sarcoplasmic reticulum and Na^+/Ca^{2+} exchanger function during early and late relaxation in ventricular myocytes. *Am. J. Physiol.* 273:H2765–H2773.